

Supplemental Information

**Characterization of a new miniCAST with diffusion flame and premixed flame options:
Generation of particles with high EC content in the size range 30 nm to 200 nm**

Michaela N. Ess and Konstantina Vasilatou

Swiss Federal Institute of Metrology, METAS, CH-3003 Bern-Wabern, Switzerland

S1 Relationship between EC/TC content and Ångström absorption exponent

Correlation of the AAE and the EC/TC content for soot generated with a) a diffusion flame and b) partially premixed flames. As visible in the two figures, the EC/TC content increases with decreasing AAE, as PAH and other organic compounds account for high wavelength dependence of the absorption due to higher absorption in the UV region. Particles composed of solely black carbon (having a high EC/TC content) exhibit an AAE of 1 or close to 1.

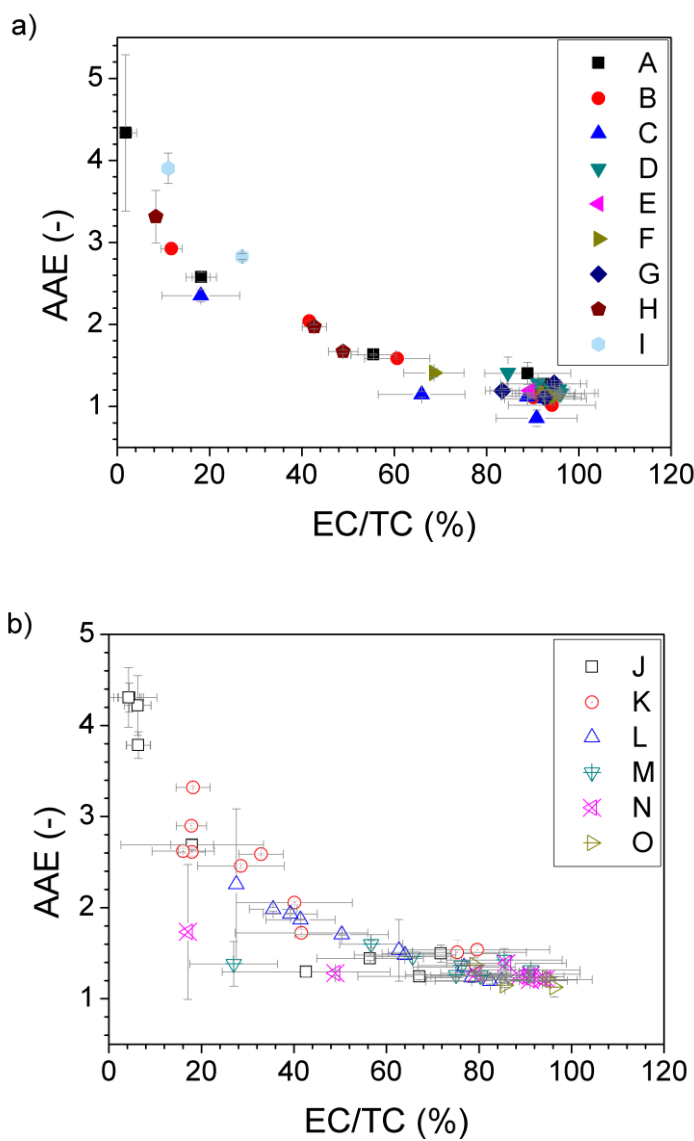


Figure S1: Correlation of the AAE and the EC/TC content for soot generated with a) a diffusion flame and b) partially premixed flames.

S2 EC/TC content and Ångström absorption exponent as function of the C/O ratio of the diffusion flame

The figures show the correlation of the AAE and the EC/TC content with the C/O ratio for soot generated with a diffusion flame in series A–I. It is clearly noticeable that for the series A–D, where the C/O ratio of the diffusion flame has been varied, the lowest AAE and the highest EC/TC content were achieved at near stoichiometric conditions. While decreasing the C/O ratio to achieve fuel-lean conditions induces just small changes, using fuel-rich conditions strongly influences the AAE and the EC/TC composition of the particles generated. In series E–I, by changing the overall gas flow in the flame at a constant C/O ratio and thus the flame size, the particles were extracted from different flame heights.

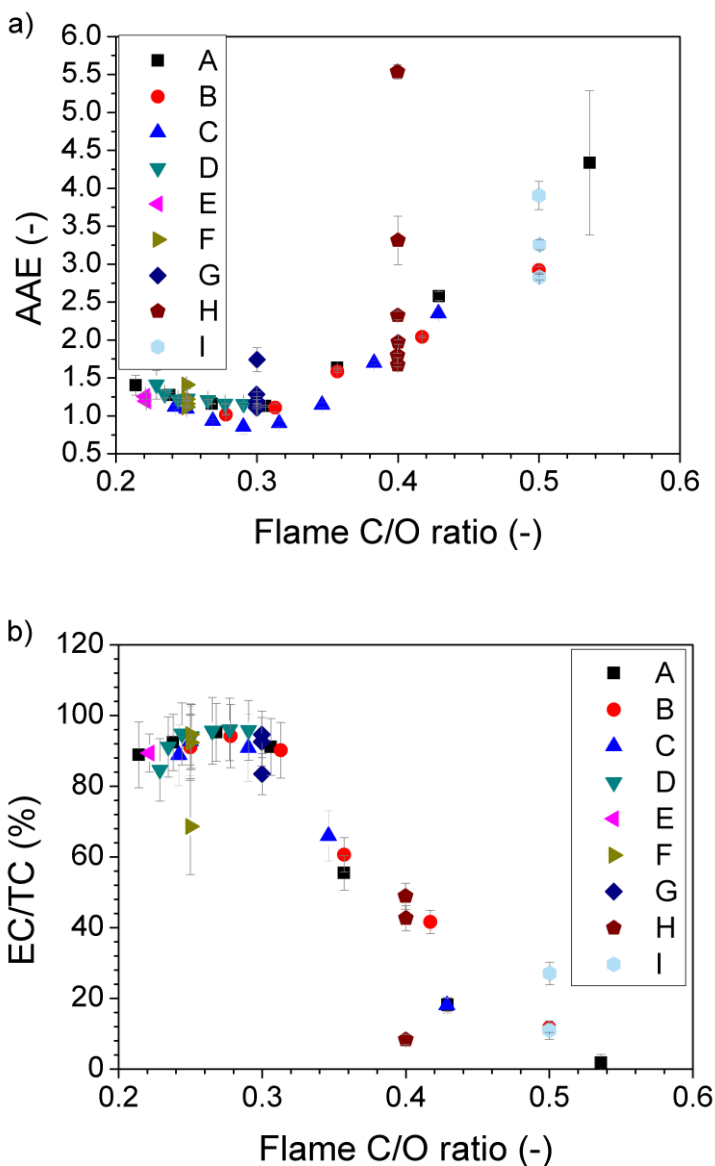


Figure S2: Correlation of the AAE and the EC/TC content with the C/O ratio for soot generated with a diffusion flame.

S3 Examples of particle number mobility size distributions

The figures display size distributions of soot generated in a diffusion flame (series A) and in a partially premixed flame (series M). Unimodal size distributions were achieved for both series. For the diffusion flame (Figure S3), as the C/O ratio decreases the GMD increases until the stoichiometric conditions are reached and thereafter decreases. At the same time the particle number concentration decreases. For the premixed flame (Figure S4), the GMD remains almost constant at first and then decreases gradually as the conditions become fuel-lean.

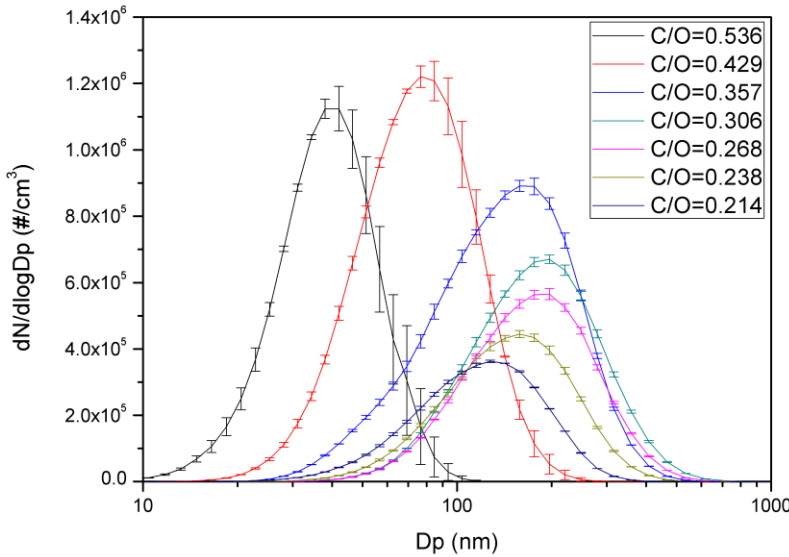


Figure S3: Size distributions of soot particles generated in series A with different C/O ratios. The soot was diluted about 1:91, the given particle concentrations have not been corrected for the dilution.

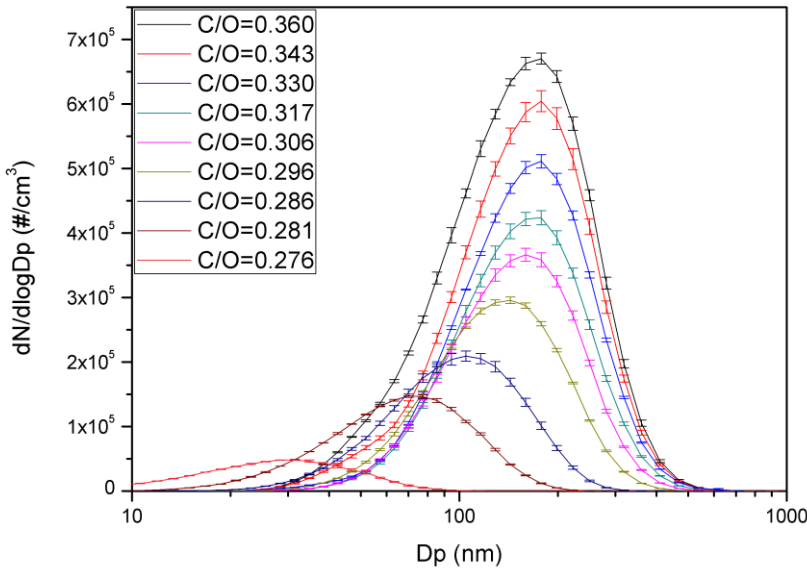


Figure S4: Size distributions of soot particles generated in series M, starting with C/O = 0.36 and adding different amount of mixing air (0–350 mL/min). The soot was diluted about 1:91, the given particle concentrations have not been corrected for the dilution.

S4 EC/TC content and Ångström absorption exponent as function of the C/O ratio of the premixed flame

The figures show the *AAE* and the EC/TC content as a function of the C/O ratio for soot generated at premixed conditions in series J–P. As in the diffusion flame the high *AAEs* and low EC/TC compositions are achieved at fuel-rich conditions, whereas soot generated in fuel-lean flames has low *AAEs* and rather high EC concentrations.

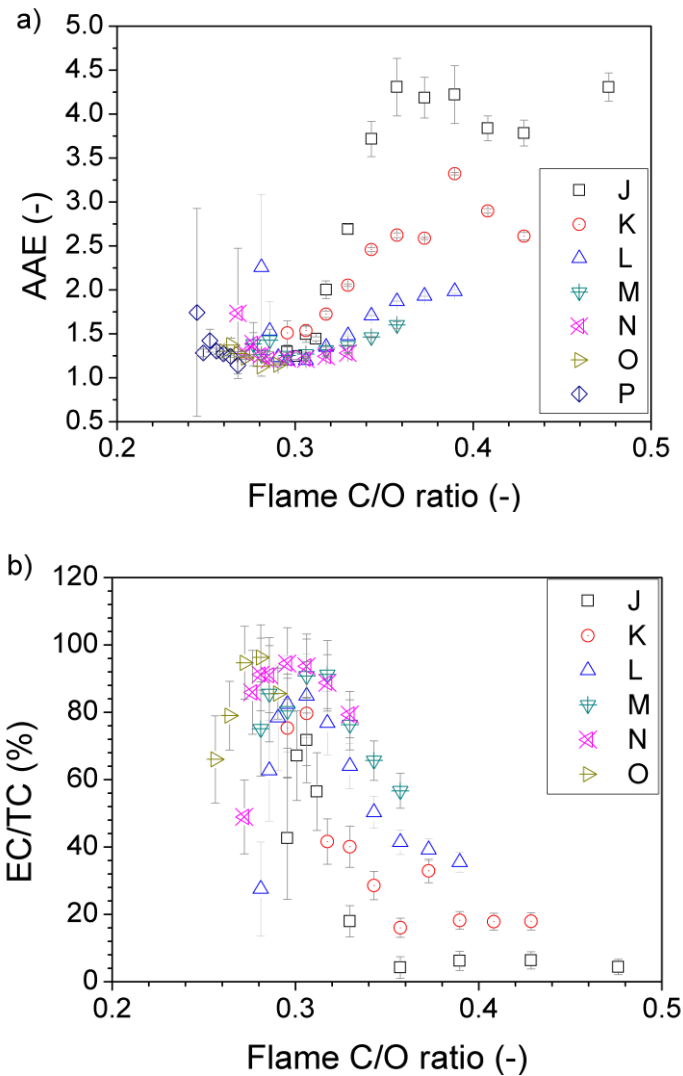


Figure S5: Correlation of the *AAE* and the EC/TC ratio with the C/O ratio for soot generated with the premixed flame.

S5 Correlation of particle size and Φ of the premixed flame

The figure shows that there is no general correlation of the GMD and the equivalent ratio Φ of the premixed flame without taking the oxygen of the surrounding oxidation air into account. This implies that the flame is not a purely premixed flame, but a combination of a premixed and diffusion flame. The oxidation air has to be taken into account when calculating the C/O ratio, since it is the overall flame composition that determines the particle properties (see Figure 4).

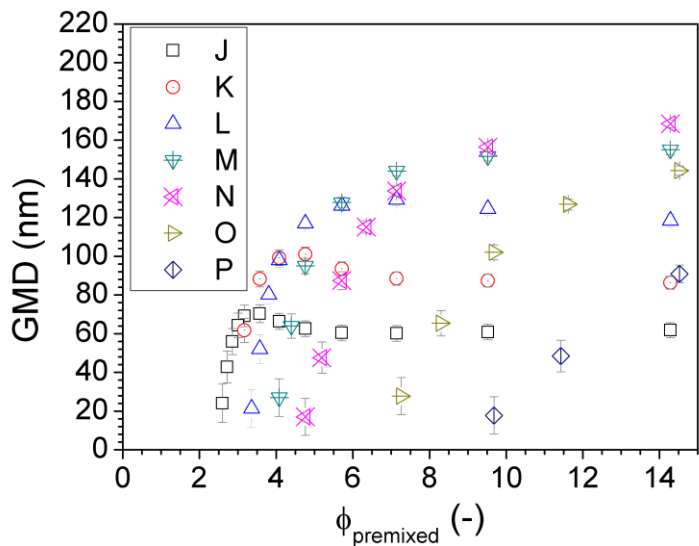


Figure S6: Correlation of the GMD with the equivalent ratio Φ of the premixed flame without taking the oxygen of the stabilizing air around in account.

S6 Influence of C/O ratio on particle number concentration and eBC mass concentration of the diffusion flame

Figure S7 shows the particle number concentration and eBC mass concentration of the series A-I of the diffusion flame. By varying the flame size (series E-I) the particle number concentration and the eBC mass concentration increase with increasing amount of propane. By increasing the C/O ratio (series A-D), the particle number concentration increases towards more fuel-rich conditions while the eBC mass concentration reaches a maximum at near stoichiometric conditions and then starts to drop. The eBC mass concentration decrease at fuel-rich conditions results mainly from the smaller particle sizes and the increase in the OC content of soot. Because of instabilities in the dilution factor and the aerosol flow, measured concentrations can vary slightly between days.

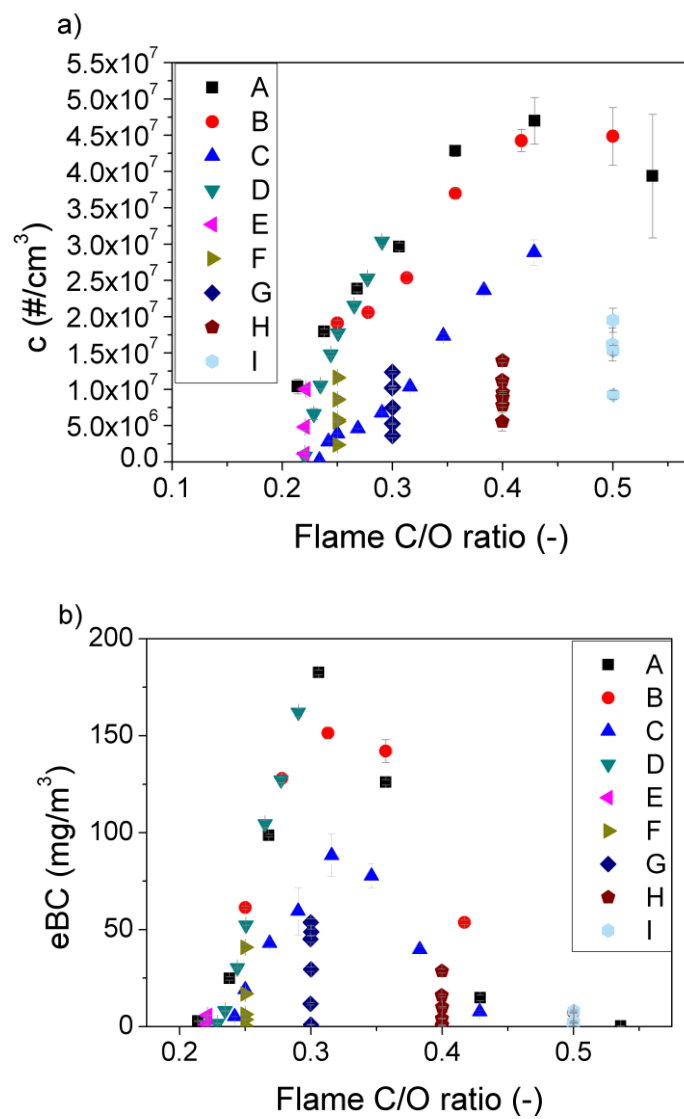


Figure S7: a) Particle number concentrations and b) eBC mass concentrations of all experiments conducted with the diffusion flame.

S7 Influence of C/O ratio on particle number concentration and eBC mass concentration of the premixed flame

Figure S8 shows the particle number concentration and eBC mass concentration of series J-P of the premixed flame. All series start at their maximal C/O ratio at diffusion flame conditions (see Figure S7). By adding premixed air in increasing amounts, the particle number and eBC mass concentration decrease rapidly for C/O ratios lower than 0.4. This is the case for all series of experiments performed with the premixed flame.

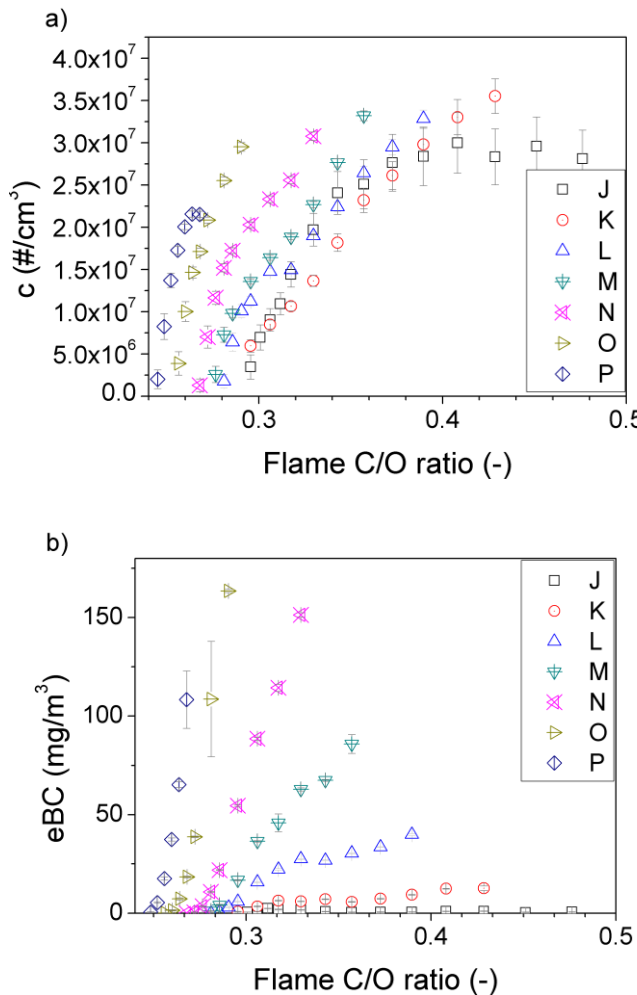


Figure S8: a) Particle number concentrations and b) eBC mass concentrations of all experiments performed with the premixed flame.

S8 Particle number and eBC mass concentrations as function of particle size.

Figure S9 shows the particle number concentration and eBC mass concentration as a function of the particle size for the diffusion flame (series A-I) and the premixed flame (series J-P). The particle number concentration and eBC mass concentration are of the same order of magnitude for the diffusion and premixed flames at each particle size. Moreover, for both diffusion and premixed flame the particle number concentration at each particle size is lower for fuel-lean conditions than for fuel-rich conditions.

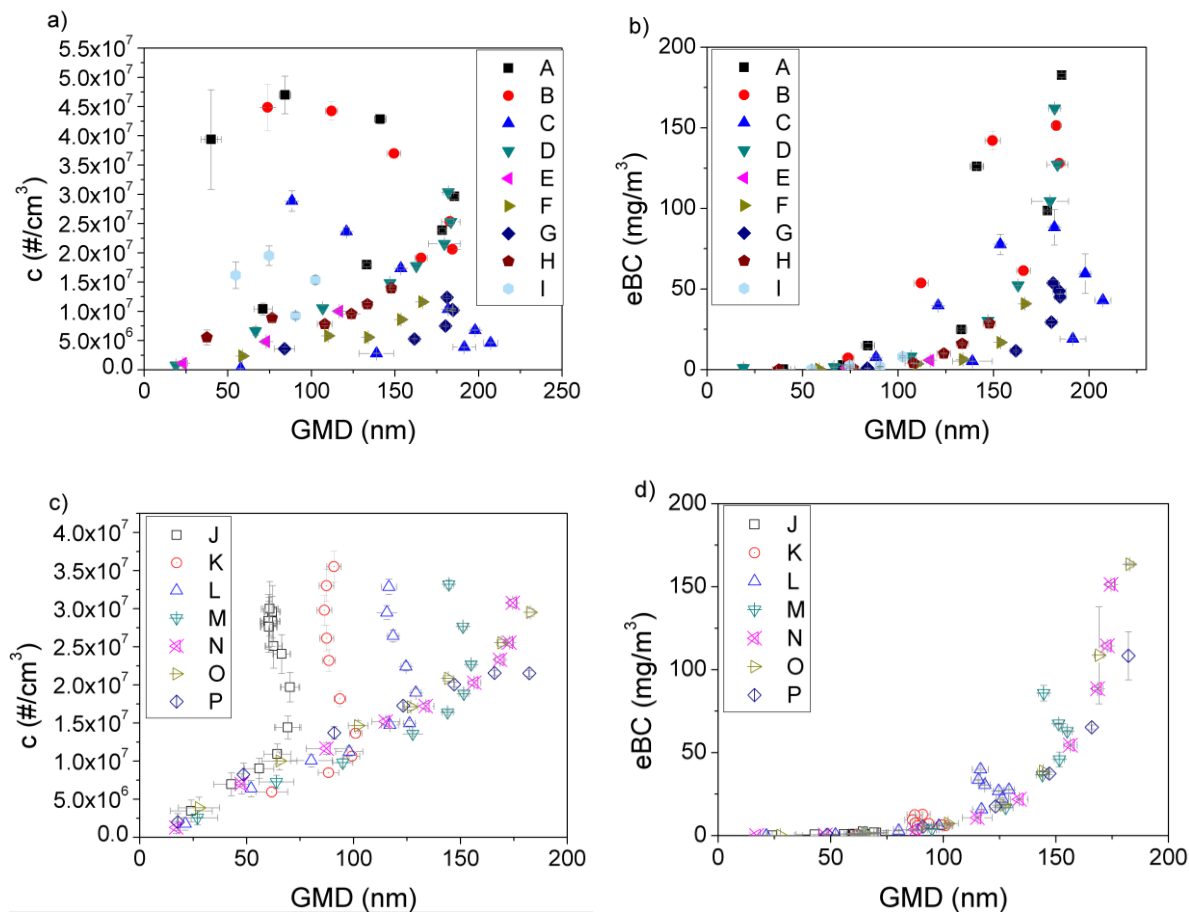


Figure S9: a) Particle number concentrations and b) eBC mass concentrations of the diffusion flame with respect to the GMD and c) particle number concentrations and d) eBC mass concentrations of the premixed flame with respect to the GMD.

S9 Effect of oxygen content in the quench gas on particle properties

The figures show that increasing the oxygen content in the quench gas from 0 to 28 % has neither an influence on the GMD nor on the EC/TC content or the AAE.

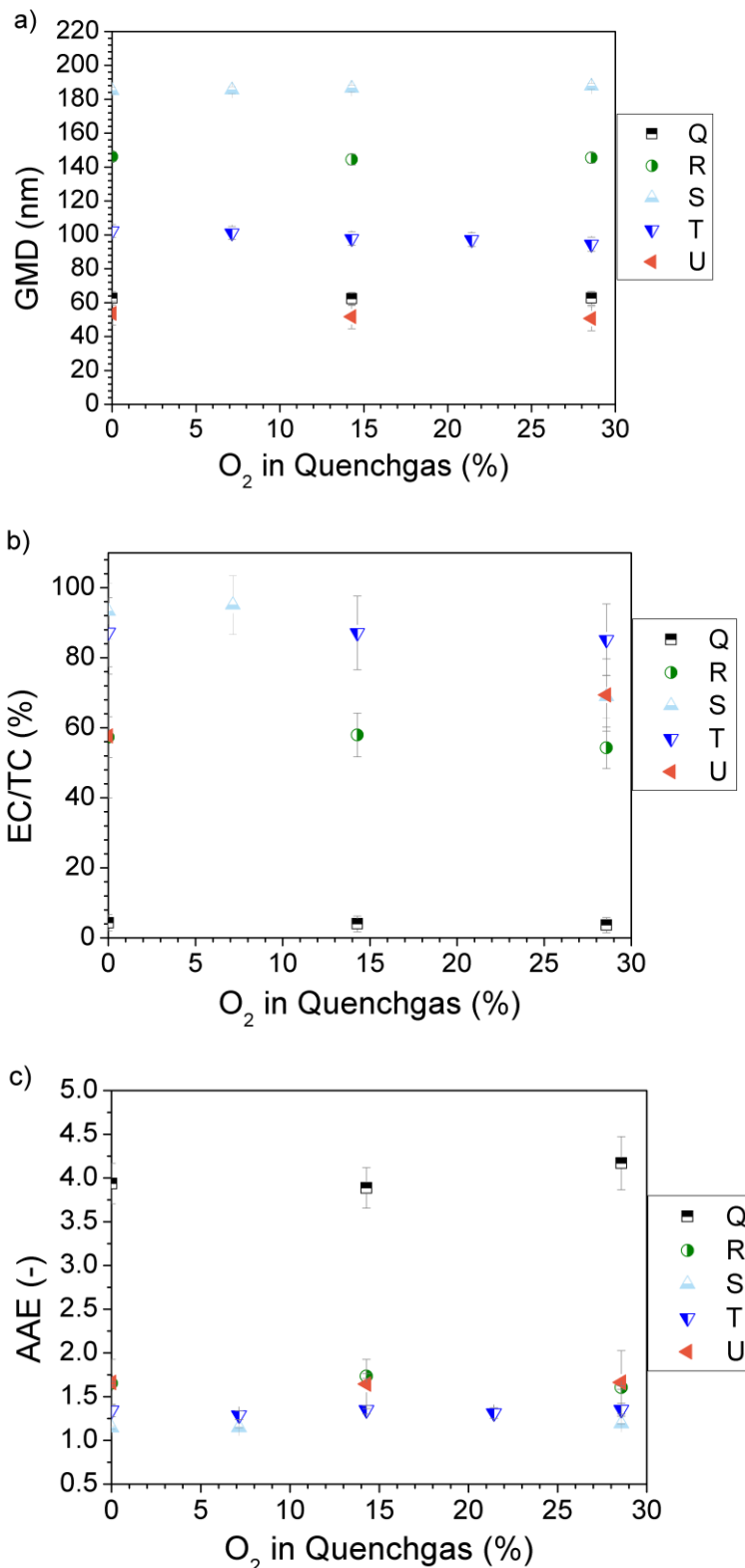


Figure S10: Influence of the oxygen content in the quench gas on particle size, composition and optical properties of soot generated at various operation conditions in series Q–U.

S10 Effect of the thermodenuder on selected operation points

The effect of the thermodenuder on particles generated in series A is displayed in Figure S 8. For particles having high EC/TC content the thermodenuder operated at 300 °C has no influence on the EC/TC content and the size distribution. For particles generated at fuel-rich conditions consisting of more OC, the treatment with the thermodenuder increases the EC/TC content by up to 20 % as some organic material is evaporated in the thermodenuder. In this case, the GMD tends to decrease.

In the current study, the bypass was chosen to have a similar inner diameter and the same retention time as the thermodenuder. Therefore particle losses and agglomeration should be the same in both cases.

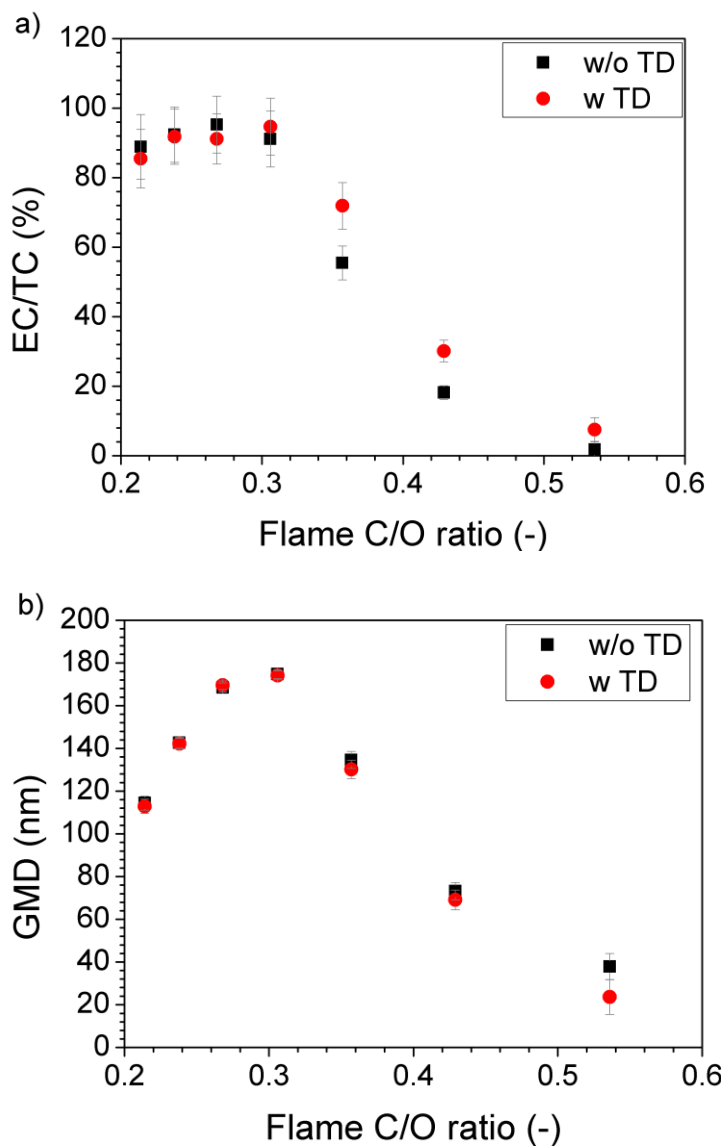


Figure S11: Effect of the usage of a thermodenuder at 300 °C on particle composition and particle size of the generated soot (series A).

S11 Gas flows of the investigated operation points and resulting particle properties

The following tables summarize the gas flows used to generate the particles in the various series, providing values for each operation point (the dilution air flow is always kept constant at 10 L/min). Additionally, the overall C/O ratio of the flame (diffusion and premixed) is given as well as particle properties, such as the GMD of the size distribution, the AAE and the EC/TC ratio for every operation point these properties were analyzed. Additionally, the particle number concentration, the eBC mass concentration and the TC mass concentration are reported assuming a constant dilution factor (91±3). The eBC/EC ratio is reported in the last column of the table. eBC was determined with the manufacturer's C-constant (1.39) and MAC value (7.77 g/m²). Since the MAC and C values are not really constant but may change with particle size and composition, the reported eBC values and eBC/TC ratios should be used with caution. When the eBC/TC ratio is marked with an asterisk, the filter-loading for the EC/OC measurement was performed on a different day than the aethalometer measurement. This implies that even when the experiments were performed under the same nominal conditions, the eBC/EC ratio may be biased due to day-to-day instabilities related to particle generation and /or the aerosol flow.

Table S1: Gas flows and particle properties of investigated diffusion flame operation points.

Series	C/O [-]	Propane [mL/min]	Oxidation air [L/min]	O ₂ to oxi- dation air [mL/min]	Premixing air [mL/min]	Quench gas [L/min]	GMD [nm]	AAE [-]	EC/TC ratio [%]	Concentration [#/cm ³]	eBC [mg/m ³]	TC [mgC/m ³]	eBC/EC [-]
A	0.536	60	0.8	0	0	7 N ₂	40±6	4.3±1.0	2±2	(3.9±0.9)·10 ⁷	0.2±0.1	6.1±0.7	1.9*
A	0.429	60	1.0	0	0	7 N ₂	84±3	2.6±0.1	18±2	(4.7±0.3)·10 ⁷	14.9±1.5	64.0±4.3	1.3*
A	0.357	60	1.2	0	0	7 N ₂	141±4	1.6±0.1	55±5	(4.3±0.1)·10 ⁷	126.0±1.4	175.7±12.5	1.3*
A	0.306	60	1.4	0	0	7 N ₂	186±2	1.1±0.1	91±8	(3.0±0.1)·10 ⁷	182.7±1.2	209.9±17.1	1.0*
A	0.268	60	1.6	0	0	7 N ₂	178±2	1.2±0.1	95±8	(2.4±0.1)·10 ⁷	98.6±0.6	119.1±8.5	0.9*
A	0.238	60	1.8	0	0	7 N ₂	133±3	1.3±0.1	92±8	(1.8±0.1)·10 ⁷	24.8±0.9	58.9±4.1	0.5*
A	0.214	60	2.0	0	0	7 N ₂	71±5	1.4±0.1	89±9	(1.0±0.6)·10 ⁷	2.9±0.3	27.2±2.4	0.1*
B	0.500	70	1.0	0	0	7 N ₂	74±4	2.9±0.1	12±1	(4.5±0.4)·10 ⁷	7.3±0.3	51.3±3.4	1.2*
B	0.417	70	1.2	0	0	7 N ₂	112±3	2.0±0.1	42±3	(4.4±0.2)·10 ⁷	53.8±1.1	156.1±9.2	0.8*
B	0.357	70	1.4	0	0	7 N ₂	149±3	1.6±0.1	61±5	(3.7±0.1)·10 ⁷	142.1±5.9	222.0±14.2	1.1*
B	0.313	70	1.6	0	0	7 N ₂	183±2	1.1±0.1	90±8	(2.5±0.1)·10 ⁷	151.4±3.0	221.4±17.9	0.8*
B	0.278	70	1.8	0	0	7 N ₂	184±2	1.0±0.1	94±9	(2.1±0.1)·10 ⁷	128.0±2.1	147.5±13.2	0.9*
B	0.250	70	2.0	0	0	7 N ₂	166±2	1.2±0.1	91±9	(1.9±0.1)·10 ⁷	61.4±0.8	75.1±7.0	0.9*
C	0.429	60	1.0	0	0	7 N ₂	88±3	2.4±0.1	18±2	(2.9±0.2)·10 ⁷	7.6±0.7	43.7±3.2	1.0
C	0.383	60	1.0	25	0	7 N ₂	121±4	1.8±0.1	-	(2.4±0.1)·10 ⁷	39.7±1.3	-	-
C	0.346	60	1.0	50	0	7 N ₂	153±4	1.3±0.1	66±7	(1.7±0.1)·10 ⁷	77.7±6.2	108.1±9.5	1.1

C	0.316	60	1.0	75	0	7 N ₂	182±2	1.0±0.1	-	(1.0±0.1)·10 ⁷	88.3±10.9	-	-
C	0.290	60	1.0	100	0	7 N ₂	198±3	1.0±0.1	91±9	(6.8±0.1)·10 ⁶	59.5±12.3	85.0±7.4	0.8
C	0.269	60	1.0	125	0	7 N ₂	207±4	1.0±0.1	-	(4.6±0.1)·10 ⁶	43.0±1.7	-	-
C	0.250	60	1.0	150	0	7 N ₂	191±2	1.2±0.1	93±10	(3.9±0.1)·10 ⁶	19.1±0.7	23.9±2.0	0.9
C	0.242	60	1.0	162	0	7 N ₂	139±3	1.2±0.1	89±9	(2.8±0.1)·10 ⁶	5.2±0.2	7.3±0.6	0.8
C	0.234	60	1.0	175	0	7 N ₂	58±14	-	-	(2.4±0.4)·10 ⁵	-	-	-
D	0.290	61	1.5	0	0	7 N ₂	182±2	1.2±0.1	96±8	(3.0±0.1)·10 ⁷	162.1±2.1	207.5±16.4	0.8
D	0.277	61	1.5	15	0	7 N ₂	183±2	1.2±0.1	96±9	(2.5±0.1)·10 ⁷	127.1±1.5	171.1±14.0	0.8
D	0.265	61	1.5	30	0	7 N ₂	180±2	1.2±0.1	96±9	(2.2±0.1)·10 ⁷	104.5±1.8	130.1±11.3	0.8
D	0.251	61	1.5	50	0	7 N ₂	163±2	1.2±0.1	94±9	(1.8±0.1)·10 ⁷	52.3±0.1	72.7±5.6	0.8
D	0.244	61	1.5	60	0	7 N ₂	147±3	1.2±0.1	95±9	(1.5±0.1)·10 ⁷	30.3±0.4	41.6±3.0	0.8
D	0.235	61	1.5	75	0	7 N ₂	107±4	1.3±0.1	91±9	(1.1±0.1)·10 ⁷	8.2±0.3	10.0±0.7	0.9
D	0.229	61	1.5	85	0	7 N ₂	67±7	1.4±0.2	85±9	(6.6±0.8)·10 ⁶	1.6±0.2	1.9±0.2	1.0
D	0.220	61	1.5	100	0	7 N ₂	19±10	-	-	(7.5±4.0)·10 ⁵	0.9±2.6	-	-
E	0.221	62	2.00	0	0	7 N ₂	117±3	1.3±0.1	89±5	(1.0±0.1)·10 ⁷	5.8±0.2	14.2±1.0	0.5
E	0.221	55	1.78	0	0	7 N ₂	73±6	1.3±0.1	-	(4.8±0.5)·10 ⁶	1.1±0.1	-	-
E	0.220	50	1.62	0	0	7 N ₂	23±10	-	-	(1.1±0.5)·10 ⁶	-	-	-
F	0.250	70	2.00	0	0	7 N ₂	166±2	1.2±0.1	95±9	(1.2±0.1)·10 ⁷	40.9±1.4	57.6±4.2	0.8
F	0.249	60	1.72	0	0	7 N ₂	154±2	1.2±0.1	-	(8.6±0.2)·10 ⁶	16.9±0.6	-	-
F	0.250	50	1.43	0	0	7 N ₂	134±3	1.2±0.1	92±8	(5.6±0.2)·10 ⁶	6.3±0.3	12.5±0.8	0.5
F	0.251	45	1.28	0	0	7 N ₂	110±4	1.3±0.1	-	(5.8±0.3)·10 ⁶	3.6±0.1	-	-
F	0.251	40	1.14	0	0	7 N ₂	59±9	1.5±0.1	69±14	(2.4±0.4)·10 ⁶	0.3±0.1	0.7±0.1	0.6
G	0.300	80	1.905	0	0	7 N ₂	181±2	1.3±0.1	83±6	(1.2±0.1)·10 ⁷	53.8±1.8	125.5±11.5	0.5
G	0.300	70	1.665	0	0	7 N ₂	184±2	1.2±0.1	-	(1.0±0.1)·10 ⁷	48.7±1.6	-	-
G	0.300	60	1.43	0	0	7 N ₂	185±2	1.2±0.1	93±7	(1.0±0.1)·10 ⁷	45.1±1.5	85.9±8.0	0.6
G	0.300	50	1.19	0	0	7 N ₂	180±2	1.3±0.1	-	(7.5±0.2)·10 ⁷	29.6±1.1	-	-
G	0.300	40	0.953	0	0	7 N ₂	162±2	1.4±0.1	95±7	(5.3±0.2)·10 ⁶	11.7±0.6	29.6±2.3	0.4
G	0.300	30	0.715	0	0	7 N ₂	84±5	1.9±0.3	-	(3.6±0.3)·10 ⁶	1.0±0.2	-	-
H	0.400	90	1.608	0	0	7 N ₂	148±3	1.8±0.1	49±4	(1.4±0.1)·10 ⁷	28.6±1.0	143.5±13.1	0.4
H	0.400	80	1.430	0	0	7 N ₂	134±3	1.9±0.1	-	(1.1±0.1)·10 ⁷	16.1±0.6	-	-
H	0.400	70	1.250	0	0	7 N ₂	124±3	2.1±0.1	43±4	(9.5±0.3)·10 ⁶	10.0±0.4	84.4±7.2	0.3
H	0.400	60	1.072	0	0	7 N ₂	108±3	2.4±0.1	-	(7.8±0.3)·10 ⁶	4.1±0.2	-	-
H	0.400	50	0.893	0	0	7 N ₂	76±3	3.3±0.4	8±1	(8.9±0.7)·10 ⁶	0.8±0.2	21.1±1.6	0.4
H	0.400	40	0.715	0	0	7 N ₂	37±6	5.6±0.1	-	(5.5±1.3)·10 ⁶	<0.1	-	-
I	0.500	90	1.285	0	0	7 N ₂	102±4	2.9±0.1	27±4	(1.5±0.1)·10 ⁷	8.0±0.5	57.6±5.0	0.5

I	0.500	80	1.142	0	0	7 N ₂	91±4	3.3±0.1	-	(9.2±0.6)·10 ⁶	1.9±0.1	-	-
I	0.500	70	1.000	0	0	7 N ₂	75±4	4.0±0.2	11±3	(2.0±0.2)·10 ⁷	2.5±0.4	27.9±2.3	0.8
I	0.500	60	0.858	0	0	7 N ₂	55±5	-	-	(1.6±0.3)·10 ⁷	-	-	-

Table S2: Gas flows and particle properties of investigated operation points with a premixed flame.

Series	C/O overall [-]	Propane [mL/min]	Oxidation air [L/min]	O ₂ to oxidation air [mL/min]	Premixing air [mL/min]	Quench gas [L/min]	GMD [nm]	AAE [-]	EC/TC ratio [%]	Concentration [#/cm ³]	eBC [mg/m ³]	TC [mgC/m ³]	eBC/EC [-]
J	0.476	60	0.9	0	0	7 N ₂	61±4	4.3±0.2	4±3	(2.8±0.4)·10 ⁷	0.6±0.1	17.4±1.6	0.8
J	0.451	60	0.9	0	50	7 N ₂	62±4	-	-	(3.0±0.4)·10 ⁷	0.4±0.2	-	-
J	0.429	60	0.9	0	100	7 N ₂	62±4	3.8±0.2	6±3	(2.8±0.4)·10 ⁷	1.0±0.1	16.6±1.6	1.0
J	0.408	60	0.9	0	150	7 N ₂	61±4	3.8±0.2	-	(3.0±0.4)·10 ⁷	0.9±0.1	-	-
J	0.390	60	0.9	0	200	7 N ₂	60±4	4.2±0.4	6±3	(2.8±0.4)·10 ⁷	0.6±0.1	14.4±1.5	0.7
J	0.373	60	0.9	0	250	7 N ₂	60±4	4.2±0.3	-	(2.8±0.4)·10 ⁷	0.6±0.1	-	-
J	0.357	60	0.9	0	300	7 N ₂	63±4	4.3±0.4	4±4	(2.5±0.3)·10 ⁷	0.5±0.2	12.0±1.3	0.9
J	0.343	60	0.9	0	350	7 N ₂	66±4	3.7±0.2	-	(2.4±0.3)·10 ⁷	0.8±0.1	-	-
J	0.330	60	0.9	0	400	7 N ₂	70±5	2.7±0.1	18±5	(2.0±0.2)·10 ⁷	1.6±0.1	9.9±1.2	0.9
J	0.317	60	0.9	0	450	7 N ₂	70±6	2.0±0.1	-	(1.4±0.2)·10 ⁷	1.8±0.2	-	-
J	0.312	60	0.9	0	475	7 N ₂	64±7	1.4±0.1	56±12	(1.1±0.2)·10 ⁷	2.4±0.1	3.6±0.5	1.2
J	0.306	60	0.9	0	500	7 N ₂	60±7	1.5±0.1	72±13	(9.0±1.3)·10 ⁶	0.9±0.1	1.9±0.3	0.7
J	0.301	60	0.9	0	525	7 N ₂	43±8	1.3±0.1	67±14	(7.0±1.5)·10 ⁶	0.6±0.1	0.7±0.1	1.3
J	0.296	60	0.9	0	550	7 N ₂	24±10	1.3±0.1	43±18	(3.5±1.4)·10 ⁶	0.1±0.1	0.2±0.1	1.2
K	0.429	60	1.0	0	0	7 N ₂	91±4	2.6±0.1	18±3	(3.6±0.2)·10 ⁷	12.6±1.2	47.6±3.8	1.5
K	0.408	60	1.0	0	50	7 N ₂	87±4	2.9±0.1	18±3	(3.3±0.3)·10 ⁷	12.4±0.2	48.6±3.8	1.4
K	0.390	60	1.0	0	100	7 N ₂	86±4	3.4±0.1	18±3	(3.0±0.2)·10 ⁷	9.4±0.2	45.9±3.7	1.1
K	0.373	60	1.0	0	150	7 N ₂	87±4	2.6±0.1	33±4	(2.6±0.2)·10 ⁷	7.4±0.2	63.5±4.7	0.4
K	0.357	60	1.0	0	200	7 N ₂	89±4	2.7±0.1	16±3	(2.3±0.2)·10 ⁷	5.7±0.2	35.5±3.1	1.0
K	0.343	60	1.0	0	250	7 N ₂	94±4	2.5±0.1	29±4	(1.8±0.1)·10 ⁷	7.1±0.2	31.8±2.9	0.8
K	0.330	60	1.0	0	300	7 N ₂	101±4	2.1±0.1	40±6	(1.4±0.1)·10 ⁷	6.0±0.1	23.9±2.5	0.6
K	0.317	60	1.0	0	350	7 N ₂	99±4	1.8±0.1	42±7	(1.1±0.1)·10 ⁷	6.4±0.2	24.2±2.7	0.6
K	0.306	60	1.0	0	400	7 N ₂	88±5	1.7±0.1	80±16	(8.5±0.6)·10 ⁶	3.4±0.2	8.1±1.3	0.5
K	0.296	60	1.0	0	450	7 N ₂	62±7	1.6±0.3	75±15	(6.0±0.8)·10 ⁶	0.8±0.1	2.0±0.3	0.5
L	0.390	60	1.1	0	0	7 N ₂	117±4	2.1±0.1	36±3	(3.3±0.1)·10 ⁷	39.9±0.5	156.3±9.5	0.7

L	0.373	60	1.1	0	50	7 N ₂	116±4	2.0±0.1	39±4	(2.9±0.1)·10 ⁷	33.6±0.2	137.0±8.5	0.6
L	0.357	60	1.1	0	100	7 N ₂	118±4	1.9±0.1	41±4	(2.6±0.1)·10 ⁷	30.5±0.2	115.0±7.6	0.6
L	0.343	60	1.1	0	150	7 N ₂	125±4	1.8±0.1	50±5	(2.2±0.1)·10 ⁷	26.8±0.2	96.1±6.9	0.6
L	0.330	60	1.1	0	200	7 N ₂	129±3	1.5±0.1	64±7	(1.9±0.1)·10 ⁷	27.6±0.2	72.8±6.0	0.6
L	0.317	60	1.1	0	250	7 N ₂	126±3	1.4±0.1	77±10	(1.5±0.1)·10 ⁷	22.3±0.4	46.0±4.5	0.6
L	0.306	60	1.1	0	300	7 N ₂	117±3	1.3±0.1	85±13	(1.5±0.1)·10 ⁷	15.7±0.2	26.8±3.2	0.7
L	0.296	60	1.1	0	350	7 N ₂	98±4	1.3±0.1	82±15	(1.1±0.1)·10 ⁷	5.9±0.2	11.7±1.6	0.6
L	0.291	60	1.1	0	375	7 N ₂	80±5	1.3±0.1	78±16	(1.0±0.1)·10 ⁷	3.0±0.2	5.0±0.8	0.8
L	0.286	60	1.1	0	400	7 N ₂	52±8	1.5±0.4	63±15	(6.4±1.1)·10 ⁶	0.5±0.1	1.4±0.3	0.6
L	0.281	60	1.1	0	425	7 N ₂	21±10	2.2±0.9	28±14	(1.8±0.8)·10 ⁶	<0.1	0.1±0.1	0.5
M	0.357	60	1.2	0	0	7 N ₂	145±4	1.6±0.1	57±6	(3.3±0.1)·10 ⁷	85.8±4.7	116.7±8.3	1.3
M	0.343	60	1.2	0	50	7 N ₂	151±4	1.5±0.1	66±6	(2.8±0.1)·10 ⁷	67.4±0.5	131.9±9.4	0.8
M	0.330	60	1.2	0	100	7 N ₂	155±3	1.4±0.1	76±8	(2.3±0.1)·10 ⁷	62.8±0.8	95.4±7.6	0.9
M	0.317	60	1.2	0	150	7 N ₂	152±3	1.3±0.1	91±10	(1.9±0.1)·10 ⁷	45.8±4.5	61.5±5.6	0.8
M	0.306	60	1.2	0	200	7 N ₂	144±3	1.3±0.1	91±11	(1.6±0.1)·10 ⁷	36.5±0.4	49.0±4.9	0.8
M	0.296	60	1.2	0	250	7 N ₂	128±3	1.3±0.1	80±11	(1.4±0.1)·10 ⁷	16.7±0.3	28.9±3.2	0.7
M	0.286	60	1.2	0	300	7 N ₂	95±4	1.4±0.2	86±15	(9.8±0.5)·10 ⁶	4.1±0.4	7.1±1.0	0.7
M	0.281	60	1.2	0	325	7 N ₂	64±7	1.3±0.1	75±14	(7.3±0.9)·10 ⁶	1.1±0.2	1.7±0.3	0.9
M	0.276	60	1.2	0	350	7 N ₂	27±10	1.4±0.3	-	(2.6±1.0)·10 ⁶	-	-	-
N	0.330	60	1.3	0	0	7 N ₂	174±3	1.3±0.1	79±7	(3.1±0.1)·10 ⁷	151.4±1.1	211.4±13.5	0.9
N	0.317	60	1.3	0	50	7 N ₂	173±2	1.2±0.1	89±9	(2.6±0.1)·10 ⁷	114.4±1.8	153.9±17.5	0.8
N	0.306	60	1.3	0	100	7 N ₂	169±3	1.2±0.1	94±10	(2.3±0.1)·10 ⁷	88.5±0.6	102.4±11.1	0.9
N	0.296	60	1.3	0	150	7 N ₂	156±3	1.2±0.1	95±11	(2.0±0.1)·10 ⁷	54.5±0.4	63.6±7.7	0.9
N	0.286	60	1.3	0	200	7 N ₂	134±3	1.2±0.1	91±11	(1.7±0.1)·10 ⁷	21.9±0.2	27.4±3.4	0.9
N	0.281	60	1.3	0	225	7 N ₂	115±4	1.3±0.1	91±11	(1.5±0.1)·10 ⁷	10.8±0.3	12.4±1.3	1.0
N	0.276	60	1.3	0	250	7 N ₂	87±5	1.4±0.2	86±13	(1.2±0.1)·10 ⁷	3.6±0.2	4.8±0.8	0.9
N	0.272	60	1.3	0	275	7 N ₂	48±8	1.3±0.1	49±11	(7.0±1.3)·10 ⁶	0.4±0.1	0.9±0.2	1.0
N	0.268	60	1.3	0	300	7 N ₂	17±10	1.7±0.8	-	(1.3±0.8)·10 ⁶	<0.1	-	-
O	0.290	61	1.5	0	0	7 N ₂	183±2	1.2±0.1	86±8	(3.0±0.1)·10 ⁷	163.5±0.8	103.5±6.8	1.8
O	0.281	61	1.5	0	50	7 N ₂	169±2	1.1±0.2	96±10	(2.6±0.1)·10 ⁷	108.7±29.3	55.8±4.3	2.0
O	0.272	61	1.5	0	100	7 N ₂	144±3	1.2±0.1	95±11	(2.1±0.1)·10 ⁷	38.7±0.4	25.2±2.3	1.6
O	0.268	61	1.5	0	125	7 N ₂	127±3	1.3±0.1	-	(1.7±0.1)·10 ⁷	18.4±0.4	-	-
O	0.264	61	1.5	0	150	7 N ₂	102±4	1.4±0.1	79±10	(1.5±0.1)·10 ⁷	7.3±0.5	7.8±0.8	1.2
O	0.260	61	1.5	0	175	7 N ₂	65±7	1.3±0.1	-	(1.0±0.2)·10 ⁷	1.4±0.3	-	-
O	0.256	61	1.5	0	200	7 N ₂	28±10	-	66±13	(3.9±1.4)·10 ⁶	<0.1	0.3±0.1	0.1

P	0.268	60	1.6	0	0	7 N ₂	182±2	1.1±0.1	-	(2.2±0.1)·10 ⁷	108.4±14.5	-	-
P	0.264	60	1.6	0	25	7 N ₂	166±3	1.2±0.1	-	(2.2±0.1)·10 ⁷	65.3±1.4	-	-
P	0.260	60	1.6	0	50	7 N ₂	147±3	1.3±0.1	-	(2.0±0.1)·10 ⁷	37.4±0.8	-	-
P	0.256	60	1.6	0	75	7 N ₂	123±3	1.3±0.1	-	(1.7±0.1)·10 ⁷	17.6±0.8	-	-
P	0.252	60	1.6	0	100	7 N ₂	91±5	1.4±0.2	-	(1.4±0.1)·10 ⁷	5.4±0.3	-	-
P	0.248	60	1.6	0	125	7 N ₂	49±9	1.3±0.1	-	(8.2±1.5)·10 ⁶	0.5±0.2	-	-
P	0.245	60	1.6	0	150	7 N ₂	18±10	1.7±1.2	-	(2.0±1.1)·10 ⁶	-	-	-

Table S3: Gas flows and particle properties of investigated operation points with oxygen in the quench gas.

Series	C/O [-]	Propane [mL/min]	Oxidation air [L/min]	O ₂ to oxi- dation air [mL/min]	Pre- mixing air [mL/min]	Quench gas [L/min]	GMD [nm]	AAE [-]	EC/TC ratio [%]	Concentration [#/cm ³]	eBC [mg/m ³]	TC [mgC/m ³]	eBC/EC [-]
Q	0.476	60	0.9	0	0	7 N ₂	63±4	3.9±0.3	4±3	(3.3±0.4)·10 ⁷	1.0±0.1	17.2±1.6	1.4
Q	0.476	60	0.9	0	0	6 N ₂ + 1 O ₂	63±4	3.9±0.3	4±3	(3.0±0.4)·10 ⁷	0.8±0.2	13.7±1.3	1.5
Q	0.476	60	0.9	0	0	5 N ₂ + 2 O ₂	63±4	4.2±0.3	4±3	(3.0±0.4)·10 ⁷	0.7±0.1	14.0±1.3	1.4
R	0.357	60	1.2	0	0	7 N ₂	146±3	1.7±0.1	57±6	(2.5±0.1)·10 ⁷	73.1±3.1	119.1±9.7	1.1
R	0.357	60	1.2	0	0	6 N ₂ + 1 O ₂	145±4	1.7±0.1	58±7	(2.2±0.1)·10 ⁷	52.1±9.6	102.0±8.7	0.9
R	0.357	60	1.2	0	0	5 N ₂ + 2 O ₂	146±4	1.6±0.1	54±6	(1.9±0.1)·10 ⁷	49.8±2.0	114.8±9.9	0.8
S	0.290	61	1.5	0	0	7 N ₂	185±2	1.2±0.1	93±8	(2.9±0.1)·10 ⁷	160.8±1.3	245.5±17.4	0.7
S	0.290	61	1.5	0	0	6.5 N ₂ +0.5 O ₂	185±2	1.2±0.1	95±9	(2.7±0.1)·10 ⁷	149.2±2.3	184.3±16.0	0.9
S	0.290	61	1.5	0	0	6 N ₂ + 1 O ₂	186±2	-	-	(2.5±0.1)·10 ⁷	-	-	-
S	0.290	61	1.5	0	0	5 N ₂ + 2 O ₂	188±2	1.2±0.1	69±6	(2.4±0.1)·10 ⁷	141.7±1.5	220.2±17.3	0.9
T	0.264	61	1.5	0	150	7 N ₂	102±4	1.3±0.1	87±10	(1.4±0.1)·10 ⁷	7.5±0.3	9.8±0.2	0.9
T	0.264	61	1.5	0	150	6.5 N ₂ +0.5 O ₂	101±4	1.3±0.1	-	(1.3±0.1)·10 ⁷	6.3±0.2	-	-
T	0.264	61	1.5	0	150	6 N ₂ + 1 O ₂	98±4	1.4±0.1	87±11	(1.3±0.1)·10 ⁷	6.6±0.1	7.5±0.1	1.0
T	0.264	61	1.5	0	150	5.5 N ₂ + 1.5 O ₂	97±4	1.3±0.1	-	(1.2±0.1)·10 ⁷	5.7±0.2	-	-
T	0.264	61	1.5	0	150	5 N ₂ + 2 O ₂	95±5	1.4±0.1	85±10	(1.2±0.1)·10 ⁷	5.4±0.2	7.3±0.1	0.9
U	0.214	60	2.0	0	0	7 N ₂	54±7	1.7±0.3	58±18	(6.1±1.0)·10 ⁶	0.7±0.2	1.2±0.3	1.0
U	0.214	60	2.0	0	0	6 N ₂ + 1 O ₂	52±8	1.6±0.3	-	(6.1±1.0)·10 ⁶	0.7±0.1	-	-
U	0.214	60	2.0	0	0	5 N ₂ + 2 O ₂	51±8	1.7±0.4	69±11	(6.1±1.0)·10 ⁶	0.6±0.1	0.8±0.1	1.0